Hepatic Medicine: Evidence and Research Dovepress

Open Access Full Text Article ORIGINAL RESEARCH

THSR Mediated *MiR374b* Targeting *C/EBP* β/*FOXO1* to Accelerate Thyroid Stimulating Hormone-Induced Hepatic Steatosis

Juyi Li[1,2], Yang Ge[3], Yuwei Chai[1], Chunjia Kou[1], Tian Tian Sun[4], Jia Liu[3,5–7], Haiqing Zhang[1,3,5–7]

[1]Department of Endocrinology, Shandong Provincial Hospital, Shandong University; Key Laboratory of Endocrine Glucose & Lipids Metabolism and Brain Aging, Ministry of Education, Jinan, Shandong, 250021, People's Republic of China; [2]Department of Endocrinology, Geriatrics Center, The First Affiliated Hospital of Anhui University of Chinese Medicine, Hefei, Anhui, 230031, People's Republic of China; [3]Department of Endocrinology, Shandong Provincial Hospital Affiliated to Shandong First Medical University, Jinan, Shandong, 250021, People's Republic of China; [4]Department of Infectious Diseases, Jinan People's Hospital, Jinan, Shandong, 271100, People's Republic of China; [5]Shandong Key Laboratory of Endocrinology and Lipid Metabolism, Jinan, Shandong, 250021, People's Republic of China; [6]Shandong Institute of Endocrine and Metabolic Diseases, Jinan, Shandong, 250021, People's Republic of China; [7]Shandong Engineering Laboratory of Prevention and Control for Endocrine and Metabolic Diseases, Jinan, Shandong, 250021, People's Republic of China

Correspondence: Jia Liu; Haiqing Zhang, Department of Endocrinology, Shandong Provincial Hospital, 324 Jingwu Road, Jinan, Shandong Province, 250021, People's Republic of China, Tel +86 18653155865; Tel +86 15168888303, Email liujia_625@163.com; zhanghq@sdu.edu.cn

Purpose: Thyroid-stimulating hormone (TSH) has been identified as an independent risk factor for non-alcoholic fatty liver disease (NAFLD), TSH binds to the TSH receptor (TSHR) to exert its function. However, the underlying mechanisms by which TSHR influences NAFLD development remain unclear. This study investigates the role of *miR374b* in NAFLD progression.

Methods: Firstly, a rat model of non-alcoholic fatty liver was constructed and divided into a normal group and a model group. The liver tissue pathology and fat accumulation were detected by Oil Red O staining and hematoxylin-eosin staining. Western blot and Real time PCR were used to detect for the impact of TSHR/miR-374b/C/EBP β/ FoxO1 pathway in the NAFLD model, and the expression of relevant inflammatory factors in each group was detected by ELISA assay. A NAFLD cell model was constructed using HepG2 cells, TSHR overexpression and interference, combined with miR-374b inhibitor and mimics, were transfected simultaneously to demonstrate TSHR/miR-374b/C/EBP β/ The mechanism of FoxO1 adipogenesis in vitro.

Results: TSHR stimulates *miR374b* secretion in human liver cancer cells (HepG2) and promotes lipid accumulation in the liver. Deficiency of *miR374b* in HepG2 cells attenuated NAFLD progression. Mechanistically, TSH increases *miR374b* expression, which then suppresses the transcription of its target genes, CCAAT/enhancer binding protein-b (*C/EBP β*) and Forkhead Box Protein O1 (*FOXO1*). This suppression influences the expression of downstream lipid metabolism proteins, including PPARγ, SREBP2, and SREBP1c. Additionally, *miR374b* directly targets the 3′UTR of *C/EBP β* and *FOXO1*, establishing a negative feedback loop in lipid metabolism.

Conclusion: These findings suggest that TSHR-induced upregulation of *miR374b* accelerates NAFLD progression by modulating lipid metabolism pathways through C/EBP β and FOXO1.

Keywords: NAFLD, *miR374b*, TSHR

Introduction

In China, non-alcoholic fatty liver disease (NAFLD) has become the most common chronic liver disease, surpassing both viral hepatitis and alcoholic liver disease.[1] Current estimates suggest a prevalence of NAFLD in the general population ranging from 15% to 33%, with rates as high as 23.3% to 59.6% among obese children and adolescents.[2]

Subclinical hypothyroidism (SCH), characterized by raised thyroid stimulating hormone (TSH) levels, is a prevalent endocrine metabolic disorder and an independent risk factor for NAFLD.[3] SCH affects approximately 4–10% of adults, increasing to 20% among women over 60 years old, and is becoming more widespread.[4] This condition is a significant contributor to secondary dyslipidemia and hypertension.[5,6] TSHR is one of the genes most closely related to GD, and

Received: 6 June 2024
Accepted: 6 November 2024
Published: 18 November 2024

Graphical Abstract

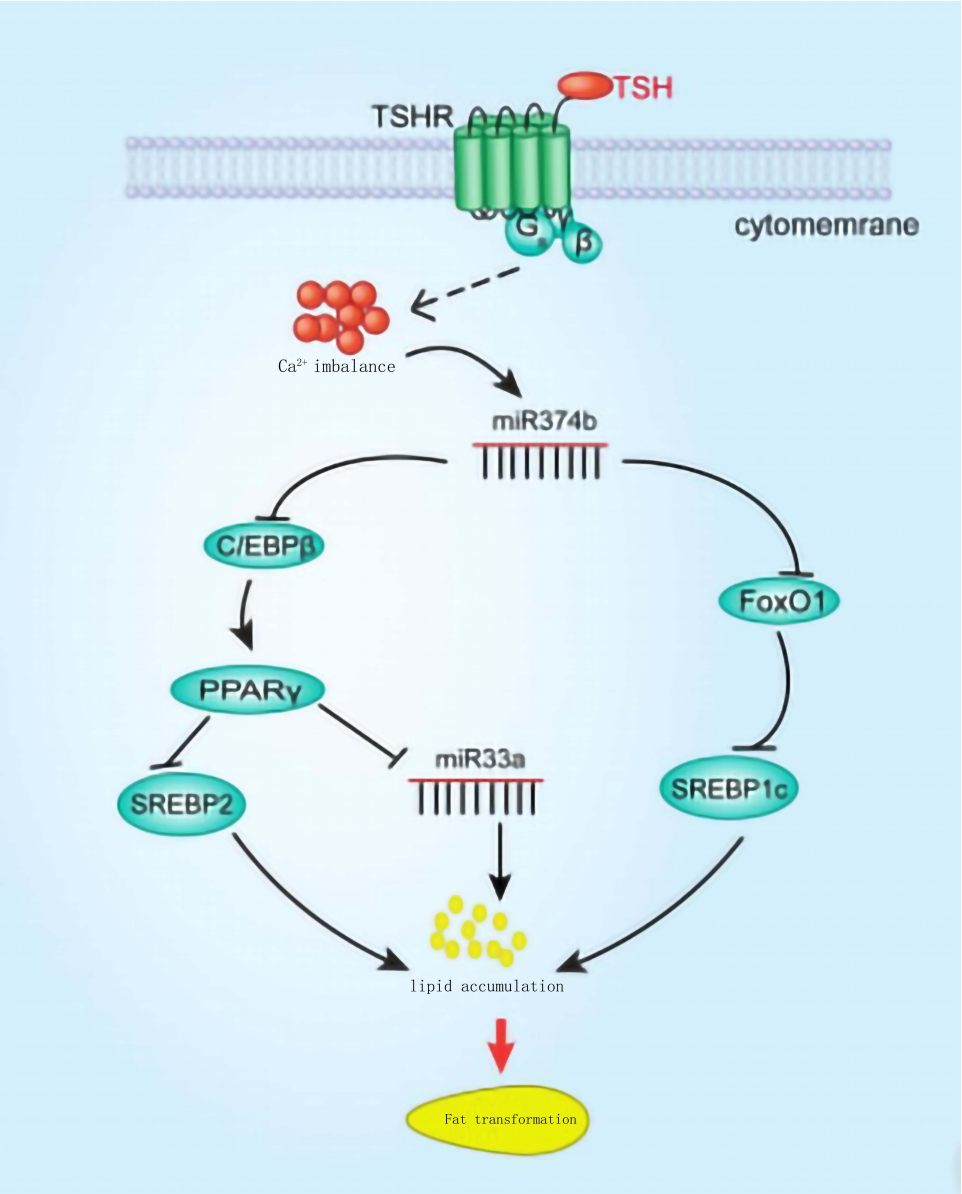

currently K1-70 has been used as a targeted TSHR inhibitor for the treatment of GD eye disease.[7] Activation of TSHR in cultured orbital fibroblasts promotes enhanced HA and fat production.[8] Despite the established association between increasing serum TSHR levels and the incidence of SCH,[9] the mechanisms by which TSHR regulates NAFLD progression remain poorly understood.

MicroRNAs (miRNAs) are known to bind specifically to the 3′ untranslated region (UTR) of target gene mRNAs, forming a complex that suppresses gene translation. Increasing evidence indicates that miRNAs play a critical role in regulating the expression of genes associated with NAFLD, with about 100 miRNAs showing significant expression differences in NAFLD patients.[10,11] These miRNAs impact various aspects of NAFLD, including glucose and lipid metabolism,[12] oxidative stress,[13] cell apoptosis,[14] inflammation, endoplasmic reticulum stress,[15] and insulin resistance.[16] For example, inhibition of *miR-33* in the liver significantly slows NAFLD progression,[17] while upregulation of *miR-122*

correlates directly with the severity of liver fibrosis in NAFLD, making it a potential biomarker and therapeutic target.[18] *MiR-34a* influences liver lipid metabolism and steatosis by targeting the transcription factor *SIRT1*.[19] Upregulated levels of *miR-378* in the liver may enhance transcription activating factor LXR α, inhibiting key enzymes and effectors in liver lipid metabolism pathways, thereby exacerbating NAFLD.[20] Furthermore, extracellular vesicles containing *miR-223* from neutrophils and other cells can decrease the expression of the pro-fibrotic gene *TAZ* in liver cells.[21] However, the specific targets of *miR374b* in SCH remain to be clarified.

Recent research indicates that *miR374b* targets CCAAT/enhancer-binding protein-b (*C/EBP β*) and Recombinant Forkhead Box Protein O1 (*FOXO1*) in adipose tissue, reducing their transcriptional stability and translational output.[22] This interaction significantly suppresses the PPAR γ signaling pathway, playing a vital role in lipid metabolism and insulin resistance. It is hypothesized that *miR374b* could be a critical miRNA in the development and progression of fatty liver disease.

Material and Methods

Animal Model

C57BL/6J mice, purchased from Hangzhou Ziyuan Laboratory Animal Technology Co., Ltd. (Hangzhou, China), underwent a 7-day acclimatization period. After that, 20 male mice were randomized into two groups: 10 mice in the control group and 10 in the model group. The model group was fed a high-fat diet for eight weeks to induce an NAFLD model. High fat feed raw material ratio, maintaining basic feed, 0.435; Lard, 0.175; Sucrose, 0.12; Whole milk powder, 0.1; Casein, 0.13; Experimental animal premix, 0.02; Calcium hydrogen phosphate, 0.02. (XTHF60, Jiangsu Xietong Pharmaceutical Bio-engineering Co., Ltd, China). The Shandong Provincial Hospital Animal Ethics Committee approved animal experiments (Ethical approval No.2021–497) in this study. Experimental animals follow the Guidelines for Ethical Review of Experimental Animal Welfare. The standard number of this guide is GB/T 35892–2018.

Cell Culture

HepG2 cells were purchased from Wuhan Pricella Biotechnology Co., Ltd. (Wuhan, China) and cultured in Dulbecco's Modified Eagle Medium (DMEM) supplemented with 10% fetal bovine serum (FBS; BIOIND Israel) in a 5% CO_2 atmosphere at 37°C.

Oil Red O Staining

HepG2 cells were washed thrice with PBS and fixed with 4% formaldehyde at room temperature for 30 minutes, followed by three additional PBS washes of 5 minutes each. Cells were then stained using an Oil Red O stain kit (Sigma Aldrich, Shanghai, China) for 1 hour after diluting the stock solution with water (3:2 ratio). After staining, cells were washed thrice with PBS (5 minutes per wash) and imaged under a microscope.

TSH/TC/TG Assay

According to the manufacturer's instructions, measure Thyroid Stimulating Hormone using a mouse/human thyroid stimulating hormone detection kit (Solarbio, China).Total cholesterol and triglyceride levels were measured using the total cholesterol/triglyceride assay kit (Solarbio, China) according to the manufacturer's instructions.

Dual-Luciferase Reporter Assay

FOXO1/C/EBPβ 3′ UTR-WT-psicheck2 and *FOXO1/C/EBPβ* 3′ UTR-Mut-psicheck2 plasmids (Limibio Co., Ltd.,China) were transfected into HepG2 cells alongside hsa-miR-374a-5p mimics or miR-NC in 24-well plates. After 48 hours, cells were lysed, and luciferase activities were measured. Firefly luciferase activity was assessed using 20μL of cracking mixture followed by 100 μL of Luc reaction solution. Renilla luciferase activity was then measured using 100μL of termination solution. The ratio of Renilla to firefly luciferase activities was calculated to determine relative luciferase activity.

Quantitative Real-Time PCR

Total RNA was extracted from HepG2 cells and tissues using TRIzol Reagent (Biosharp, China). RNA concentration was measured with a Nanodrop 2000 spectrophotometer (Thermo Fisher Scientific, USA). Reverse transcription was performed using Hifair III first strand cDNA Synthesis SuperMix (Yeasen Biotechnology Co., Ltd., China). qPCR was conducted using Hieff UNICON® Universal Blue qPCR SYBR Master Mix (Yeasen Biotechnology Co. Ltd., China) on a LightCycler480 Real-Time fluorescence quantitative PCR instrument (Roche, Switzerland). The gene primers used in the experiment are shown in Table 1.The thermal cycling conditions were: 1 cycle at 95°C for 2 minutes, followed by 40 cycles at 95°C for 15 seconds and 60°C for 20 seconds, then 95°C for 15 seconds and 60°C for 60 seconds. β-actin was used as an internal control, and each sample was tested in triplicate.

Table 1 Specific Primer Sequences for qRT-PCR

Primer Name	Sequence (5′-3′)	Primer Length (bp)	Product Size (bp)
Mouse-β-actin F	GTGACGTTGACATCCGTAAAGA	22	245
Mouse-β-actin R	GCCGGACTCATCGTACTCC	19	
Mouse-TSHR-F	ACCCTGATGCCTTGACAGAG	20	174
Mouse-TSHR-R	ATAGGCCCTGGAATGCGTTT	20	
Mouse-C/ebpβ-F	GAGCGACGAGTACAAGATGC	20	150
Mouse-C/ebpβ-R	AGCTGCTCCACCTTCTTCTG	20	
Mouse-foxo1-F	CCATTGCGGAAAGAGAGAGC	20	184
Mouse-foxo1-R	CTGCCCATGATTCACACTGG	20	
Mouse-pparγ-F	GACAGGAGCCTGTGAGACCA	20	113
Mouse-pparγ-R	TCACCGCTTCTTTCAAATCTTGT	23	
Mouse-SREBP2-F	CAGCTGGATCCTCCCAAAGA	20	149
Mouse-SREBP2-R	CTCAGAACGCCAGACTTGTG	20	
Mouse-SREBP1c-F	ACACTTCTGGAGACATCGCA	20	159
Mouse-SREBP1c-R	CGGATGAGGTTCCAAAGCAG	20	
U6-f	CTCGCTTCGGCAGCACA	17	94
U6-r/rt	AACGCTTCACGAATTTGCGT	20	
Mouse-mir-374b-5p F	GCGCGATATAATACAACCTGC	21	66
Mouse-mir-374b-5p RT	GTCGTATCCAGTGCAGGGTCCGAGGTATTCGCACTGGATACGACCACTTA	50	
Mouse-mir-33-3p F	CGCGCAATGTTTCCACAGTG	20	66
Mouse-mir-33-3p RT	GTCGTATCCAGTGCAGGGTCCGAGGTATTCGCACTGGATACGACGTGATG	50	
Mouse-mir-R	AGTGCAGGGTCCGAGGTATT	20	
Human-β-actin F	GGGCATGGGTCAGAAGGATT	20	81
Human-β-actin R	TCGATGGGGTACTTCAGGGT	20	
Human-C/ebpβ F	CTCTCTGCTTCTCCCTCTGC	20	173
Human-C/ebpβ R	ACAAGCCCGTAGGAACATCT	20	
Human-foxo1 F	GTGTCAGGCTGAGGGTTAGT	20	177
Human-foxo1 R	CTGCCAAGTCTGACGAAAGG	20	
Human-pparγ F	ACAGATCCAGTGGTTGCAGA	20	155
Human-pparγ R	ATTGCCATGAGGGAGTTGGA	20	
Human-SREBP2 F	ACCTGTGACCTGCTACTGTC	20	180
Human-SREBP2 R	CAGGAACACCTTGCGGTATG	20	
Human-SREBP1c F	GGGTCAGTTGTCCCTTCTCA	20	141
Human-SREBP1c R	TGAGACGTGCCAGACTTCTT	20	
U6-f	CTCGCTTCGGCAGCACA	17	94
U6-r/rt	AACGCTTCACGAATTTGCGT	20	
Human-mir-374b-5p F	GCGCGATATAATACAACCTGC	21	66
Human-mir-374b-5p RT	GTCGTATCCAGTGCAGGGTCCGAGGTATTCGCACTGGATACGACCACTTA	50	
Human-mir-33a-3p F	CGCGCAATGTTTCCACAGTG	20	66
Human-mir-33a-3p RT	GTCGTATCCAGTGCAGGGTCCGAGGTATTCGCACTGGATACGACGTGATG	50	
Human-miR R	AGTGCAGGGTCCGAGGTATT	20	

Western Blot

Protein extraction was conducted using a total protein extraction kit (Solarbio, China), and protein concentrations were determined with a BCA protein assay kit (Solarbio, China). For electrophoresis, 20 μg of protein per sample was separated on a 10% SDS-PAGE and transferred to a polyvinylidene fluoride (PVDF) membrane. The membrane was blocked with 5% skim milk for 1 hour at room temperature, incubated overnight at 4°C with primary antibodies, followed by a 1.5-hour room temperature incubation with corresponding secondary antibodies. Immunoblots were scanned in grayscale, using β-actin as an internal reference protein.Information on the use of the antibodies is provided in Table 2.

Statistical Analysis

Statistical analyses were performed using SPSS version 21.0 (IBM, USA). Data were analyzed using the *t*-test and expressed as mean ± standard deviation (SD). Differences were considered statistically significant at $P<0.05$ and marked accordingly in the results.

Results

Effect of TSH on Adipose Degeneration in HepG2 Cells

In order to understand the role of TSH in the occurrence and development of NAFLD, ELISA was used to detect the concentration of TSH in the serum of NAFLD mouse models. The results showed that TSH was significantly over-expressed in this group (Figure 1A). In vitro, HepG2 cells were treated with varying concentrations of TSH, and lipid accumulation was assessed using oil red staining. As depicted in Figure 1B, lipid levels were significantly higher in the TSH-treated group than in controls, increasing progressively with rising TSH concentrations. At the same time, levels of total cholesterol (TC) and triglycerides (TG) were elevated in cells treated with TSH (Figure 1C). While TC levels at a 1μM concentration of TSH did not differ significantly from controls, TG levels significantly increased, particularly at a 4μM concentration. Importantly, *miR374b* expression was found to correlate positively with TSH concentration (Figure 1D), suggesting that TSH induces *miR374b* expression in HepG2 cells.

TSH-Induced Hepatic Steatosis in HepG2 Cells Dependent on TSHR

To determine if TSH expression depends on TSHR, three siRNAs targeting the *TSHR* gene in HepG2 cells were designed. Effective knockdown was achieved with sequences TSHR-Si-385 (CGGAAUACCAGGAACUUAATT) and TSHR-Si-656 (GGACAAAGCUGGAUGUGUGUGUGUGUTT), which reduced *TSHR* expression by 70% and 50%, respectively (Figure 2A). TSHR-Si-385 was used for further experiments to knock down *TSHR*, and recombinant TSH protein was employed for intervention treatments. The Oil Red O staining results, as shown in Figure 2B, showed no significant lipid accumulation in the OE-NC and si NC groups compared to the Control group. The OE-TSHR group showed a significant increase in lipids compared to the OE-NC group, while the si TSHR group showed a decrease in lipid content compared to the si NC group; After TSH treatment of cells, the lipid content of OE-NC+TSH and si-NC +TSH significantly increased; The OE-TSHR+TSH group had the highest lipid content, significantly higher than the lipid content of cells treated with a single treatment; The lipid content of the si TSHR+TSH group was significantly increased compared to the si TSHR group, indicating that TSH promotes liver lipid accumulation in a TSHR dependent manner.

Table 2 Information on the Use of the Antibodies

Antibody	Factory	Cat No	Host	Dilution Ratio	Formula Weight (kDa)
C/EBPβ	Proteintech	23431-1-AP	Rabbit	1:1k	36
FoxO1	Proteintech	18592-1-AP	Rabbit	1:1k	70–80
PPARγ	Proteintech	22061-1-AP	Rabbit	1:1k	66–70
SREBP2	Proteintech	28212-1-AP	Rabbit	1:1k	124
SREBP1c	Proteintech	14088-1-AP	Rabbit	1:1k	125
β-actin	Proteintech	20536-1-AP	Rabbit	1:2k	42
HRP-conjugated Goat Anti-Rabbit IgG (H+L)	Proteintech	SA00001-2	Goat	1:10k	

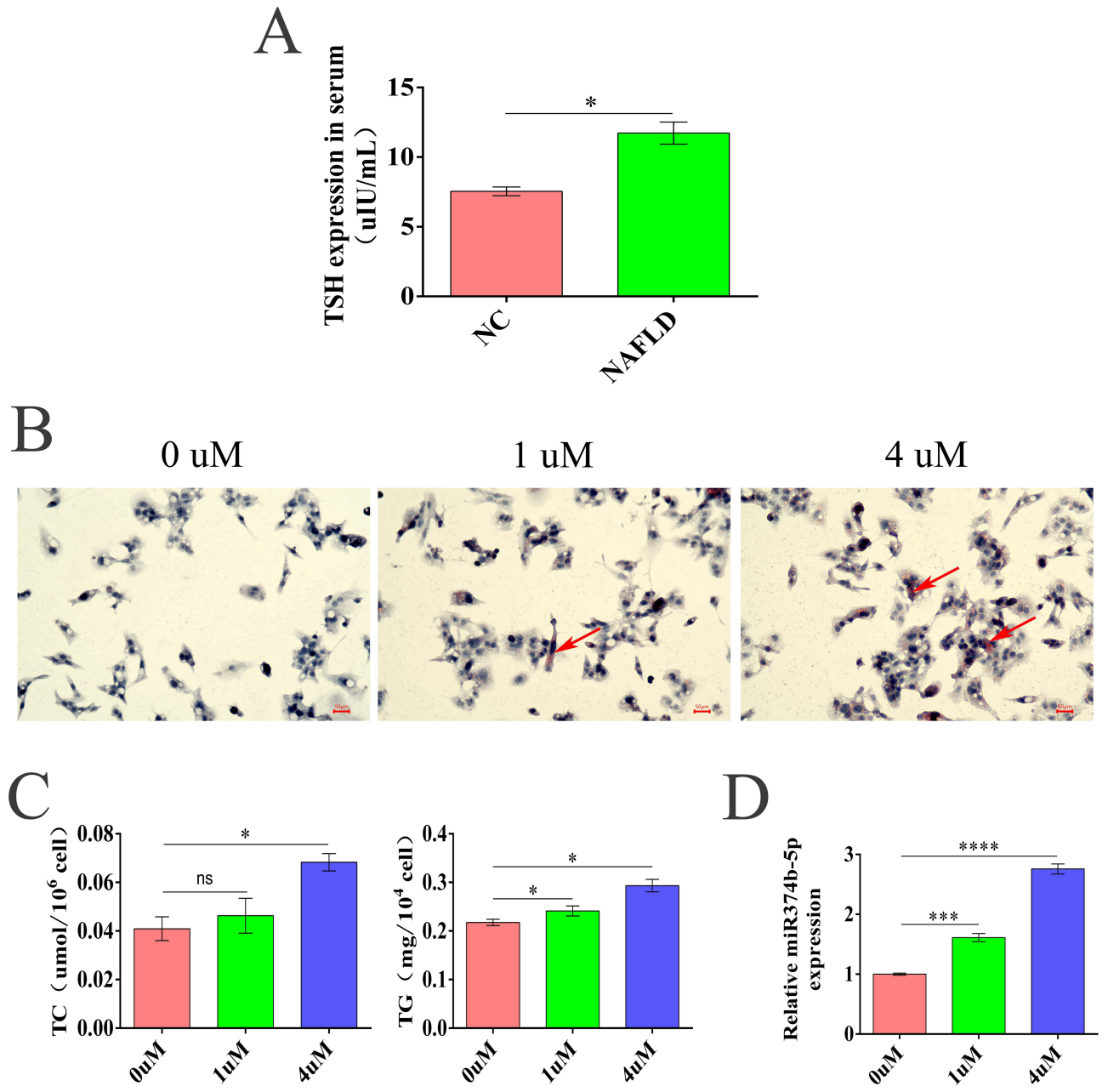

Figure 1 Effect of TSH on adipose degeneration in HepG2 cells. (**A**) Comparison of serum TSH levels between NAFLD mouse model and control group (n=3, * $P < 0.05$). (**B**) Oil red O staining of HepG2 cells treated with TSH (0 μM, 1 μM, 2 μM) (n=3), Scale bar = 50 μm. (**C**) Changes of serum TC and TG levels in each group treated with TSH (0 μM, 1 μM, 2 μM) (n=3, one-way ANOVA and Tukey's multiple comparison test; ns, nonsignificant; * $P < 0.05$ versus 0 μM). **(D)** The expression of *miR-374b-5p* in each group compared with control (n=3, *** $P < 0.001$ versus 0 μM, **** $P < 0.0001$ versus 0 μM).

Additionally, levels of TC and TG correlated with *TSHR* expression, increasing in the *TSHR* overexpression group (Figure 2C). Real-time quantitative PCR analysis demonstrated that both *TSH* and *TSHR* overexpression could upregulate *miR-374b* expression. Notably, even after *TSHR* knockdown, TSH overexpression still elevated *miR-374b* levels (Figure 2D), indicating that *miR-374b* expression is primarily regulated by TSH, with *TSHR* exerting a regulatory effect.

Effect of miR374b on the Regulation of the Transcription Factor C/EBP β and FOXO1 Expression

To delineate the gene regulatory function of *miR374b* in NAFLD, gene manipulation was conducted on *miR374b*, with both mimics and inhibitors synthesized and transfected into HepG2 cells. *C/EBP β, FoxO1, PPAR γ, SREBP2*, and

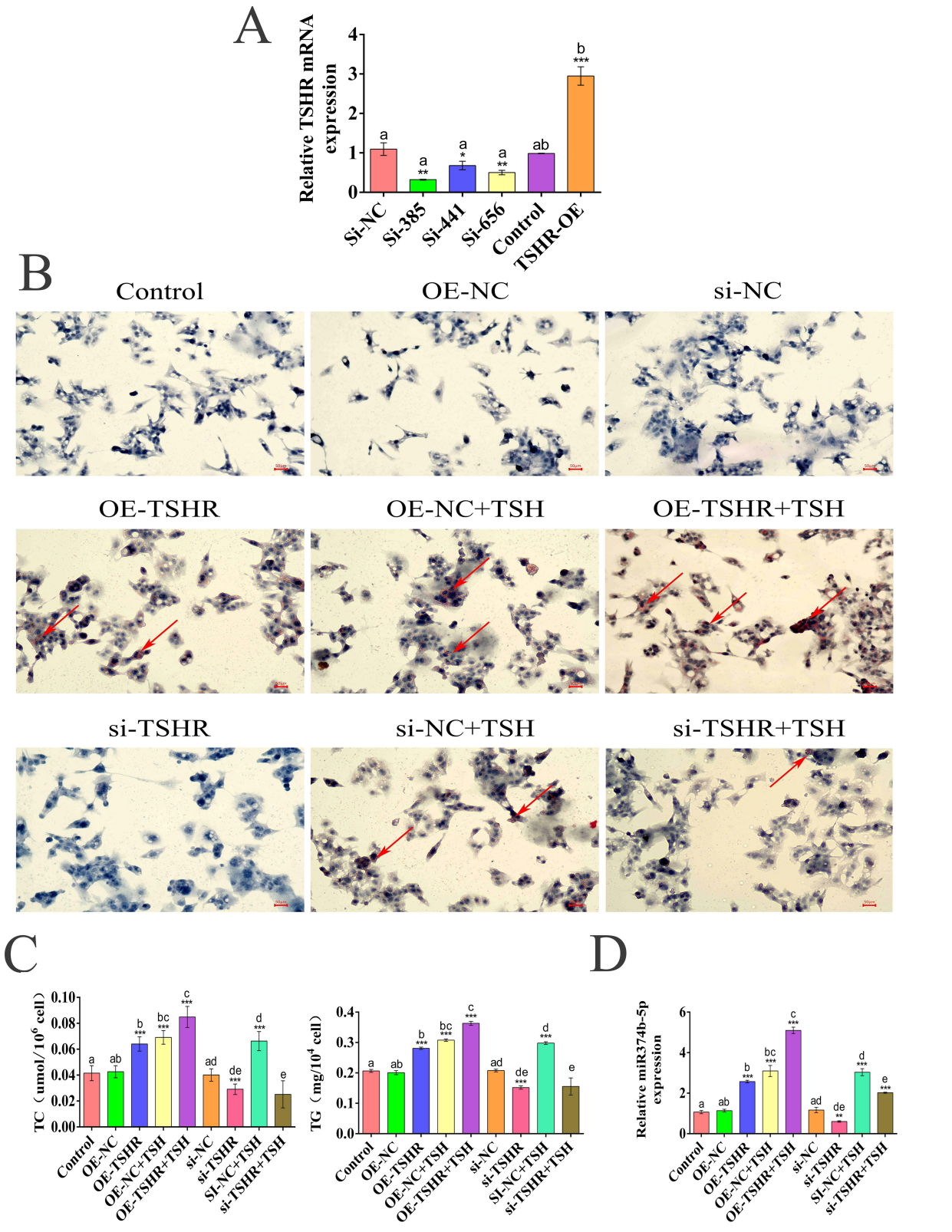

Figure 2 TSH-induced hepatic steatosis in HepG2 cells dependent on TSHR. (**A**) Comparison of TSHR mRNA expression levels between the interference and overexpression TSHR groups and the control group (n=3,* $P < 0.05$; ** $P < 0.01$; *** $P < 0.01$). (**B**) Oil red O staining of HepG2 cells treated with TSHR combined with TSH (2 μM) (n=3,Red arrow lipid accumulation site,Scale bar = 50 μm. (**C**) Changes of serum TC and TG levels in each group treated with TSHR-siRNA and TSH (2 μM) (n=3;*** $P < 0.001$). (**D**) The expression of *miR-374b*-5p in each group checked by Realtime-PCR (n=3; **$P < 0.01$; ***$P < 0.001$).

https://doi.org/10.2147/HMER.S481687 DovePress

SREBP1c expression levels were assessed using real-time qPCR. Results showed a decrease in the expression of *C/EBP β, PPAR γ*, and *FoxO1* following *miR374b* upregulation, while *miR-33, SREBP2*, and *SREBP1c* expression significantly increased (Figure 3A). In contrast, *miR374b* knockdown elevated *C/EBP β, PPAR γ*, and *FoxO1* expression and reduced *miR-33, SREBP2*, and *SREBP1c*. Western blot analysis corroborated the qPCR findings, confirming the regulatory effects at both protein and mRNA levels (Figure 3B), thus indicating *miR374b*'s role in modulating the expression of these key metabolic regulators.

MiR374b Regulates NAFLD by Targeting C/EBPβ and FOXO1

To elucidate the role of *miR374b* in NAFLD, we regulated *miR374b* expression in a TSH-induced HepG2 cell model by constructing *miR374b* mimics and inhibitors. Functional validation via oil red staining demonstrated that overexpression of *miR374b* enhanced lipid accumulation while its knockdown decreased lipid levels (Figure 4A). This effect was exacerbated with TSH intervention, though fat accumulation was significantly reduced in the *miR374b* knockdown group compared to controls, suggesting that *miR374b* operates independently of TSH in influencing NAFLD. Biochemical assays confirmed that *miR374b* overexpression increased TC and TG, which were reduced upon *miR374b* knockdown (Figure 4B). *C/EBP β* and *FOXO1* were identified as target genes of *miR374b*, both containing binding sites within their 3′UTR regions, confirmed via dual-luciferase reporter assays (Figure 4C and D). Real-time qPCR analysis revealed that upregulation of *miR374b* decreased the expression of *C/EBP β, FOXO1*, and *PPAR γ*, while *miR-33, SREBP2*, and *SREBP1c* expressions were elevated. Conversely, *miR374b* knockdown led to increased expression of *C/EBP β* and slight changes in *FOXO1* and *PPAR γ* (Figure 4E). Western blot analysis corroborated these findings (Figure 4F), underscoring *miR374b*'s role in targeting and suppressing *C/EBP β* and *FOXO1* expression, impacting lipid metabolism in NAFLD.

Effect of miR374b on the Regulation of NAFLD in vivo

An NAFLD mouse model was replicated, and fatty lesions in the liver tissues of the model mice were identified via HE pathological staining (Figure 5A). Oil red O staining indicated a significant accumulation of adipocytes in the liver tissues of NAFLD mice (Figure 5B). Quantitative analyses of TC and TG in serum and liver tissues showed elevated levels in the model group compared to the control group. TSH levels were significantly increased in the model group, as illustrated in Figure 5C. qPCR analysis detected upregulated expression of *TSHR* and *miR-374b* in the model group (Figure 5D), indicating that *TSHR* promotes the expression of *miR-374b*. As a target gene of *miR-374b, C/EBP β* expression was reduced, leading to downregulation of the transcription factor *FOXO1* and its downstream target genes. Western blot analyses corroborated the qPCR findings (Figure 5E). In line with prior studies, an increase in *miR-33-3p* expression was observed, which may be associated with the regulation of *SREBP1*. Collectively, these findings suggest that TSH upregulates *miR374b* expression via TSHR in liver cells, which then influences C/EBP β and modulates critical molecules in lipid metabolism, thereby promoting lipid accumulation in liver cells and inducing hepatic steatosis.

Discussion

TSH, a key protein in SCH lesions, is involved in inducing NAFLD through its interaction with the TSH receptor (TSHR).[23] TSH regulates thyroid activity and comprehensively activates thyroid metabolism,[24] including the synthesis of thyroid-specific proteins such as thyroglobulin (Tg), thyroid peroxidase (TPO), and the sodium-iodide symporter (NIS). Thyroid hormone receptors (TRs), TRα and TRβ, bind with Thyroid hormone (3,5,3′-triiodothyronine, T3) to regulate gene expression associated with TSH.[25] Beyond its thyroid-specific roles, TSH influences various hepatic metabolic activities, promoting lipid output, oxidation, and *de novo* adipogenesis.[26] The TSH/TSHR signaling pathway is crucial for the morphogenesis and differentiation of embryonic glands in mice,[27] affecting lipid metabolism through modulation of AMPK and PPARα signal transduction.[28,29] However, the relationship between TSH and miRNAs has not yet been elucidated.

This study elucidates the novel role of *miR374b* in the pathogenesis of NAFLD mediated by TSH. The results demonstrate that *miR374b* significantly influences lipid metabolism and regulates FOXO1 and its downstream target genes in HepG2 cells. MiR374b is involved in the complex regulation of NAFLD lipid metabolism. Notably, *miR374b* activity is significantly elevated in a NAFLD mouse model; TSH promotes its expression via the TSHR. Moreover,

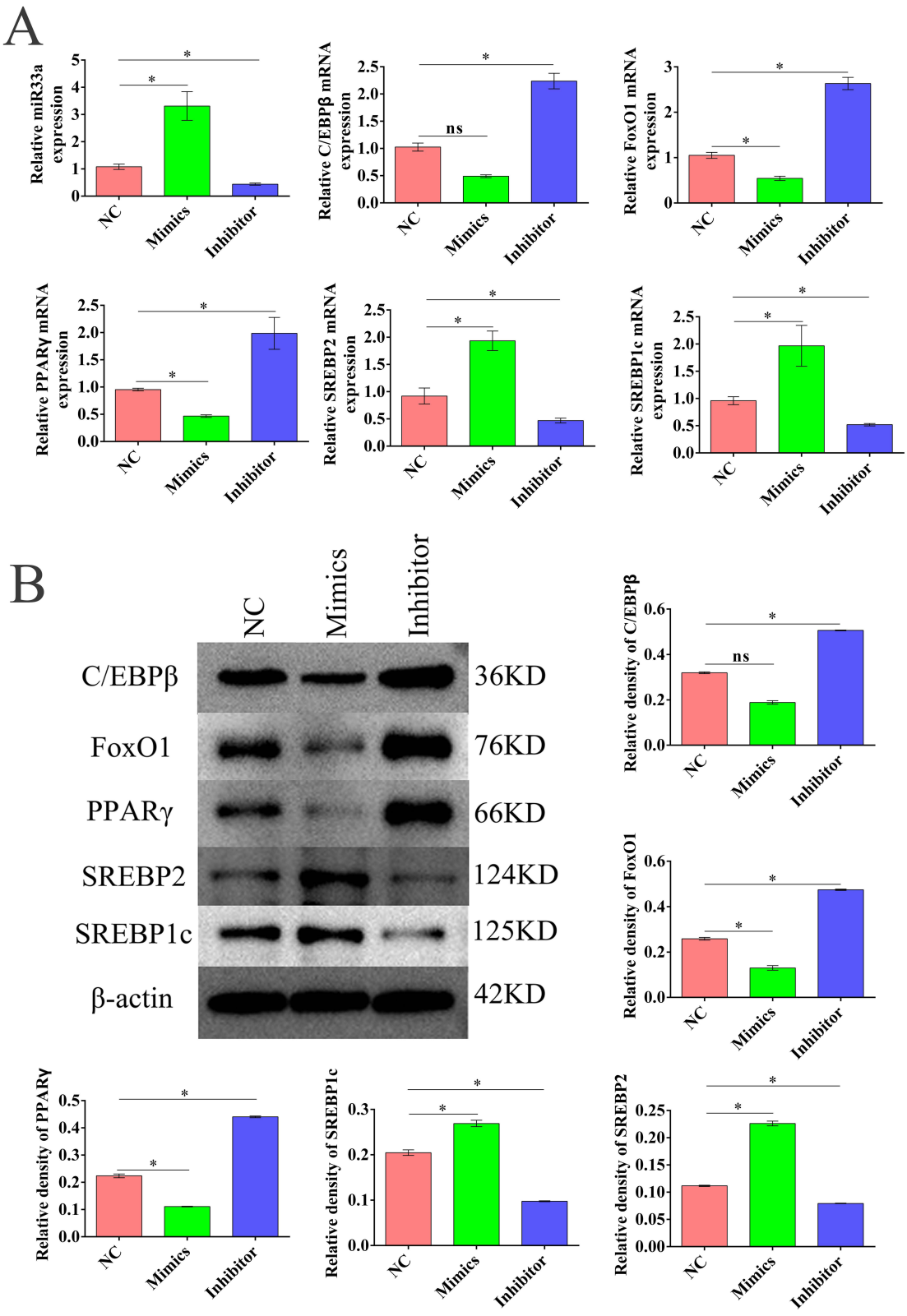

Figure 3 Effect of miR374b on the regulation of the transcription factor *C/EBP β* and *FOXO1* expression. (**A**) The mRNA expression of *C/EBP β, FoxO1, PPAR γ, SREBP2, SREBP1c*, and *miR33a* in each group compared with the normal control (n=3,* $P < 0.05$). (**B**) Western blot showing the expression of TSHR, C/EBPβ, FOXO1, PPARγ, SREBP2, and SREBP1c in each group compared with normal control (n=3,* $P < 0.05$).

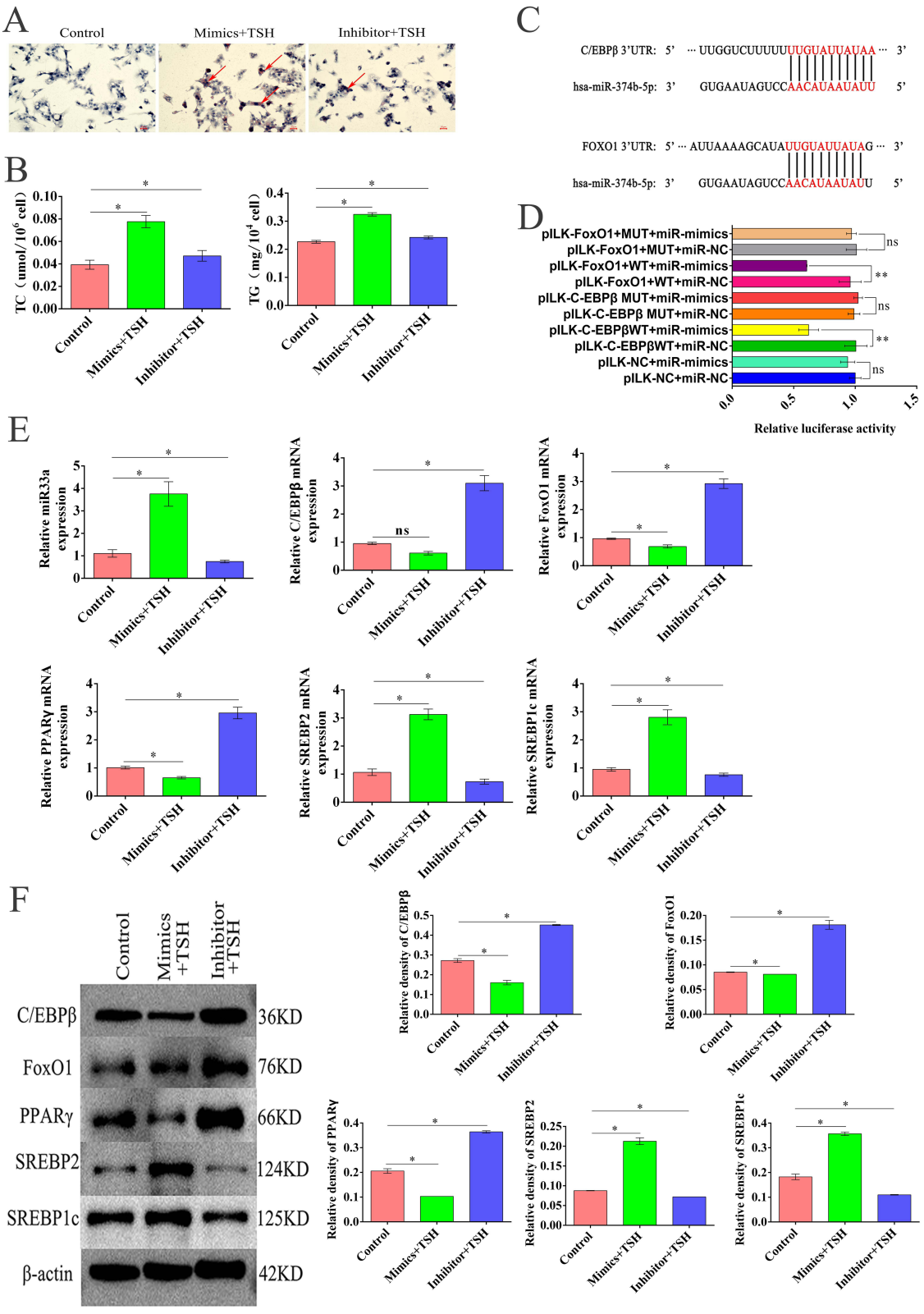

Figure 4 *MiR374b* regulates NAFLD by targeting *C/EBP β* and *FOXO 1*. (**A**) Oil red O staining of HepG2 cells transfected with *miR374b* mimics and inhibitor (n=3), Scale bar = 50 μm. (**B**) Changes of serum TC and TG levels in each group treated with *miR374b* mimics and inhibitors combined with TSH (2 μM) (n=3,* $P < 0.05$ versus control). (**C**) Predicted binding sites with *C/EBP β* and *FOXO1*. (**D**) The dual luciferase reporter gene assay confirmed the binding of *miR374b* to *C/EBP β* and *FOXO1* genes; Error bars indicate the mean ± SD; ** $P < 0.01$, (**E**) The mRNA expression of *C/EBP β, FoxO1, PPAR γ, SREBP2, SREBP1c*, and *miR33a* in each group compared with normal control (n=3,* $P < 0.05$). (**F**) Western blot showed the expression of TSHR, C/EBPβ, FOXO1, PPARγ, SREBP2, and SREBP1c in each group compared with normal control (n=3, * $P < 0.05$).

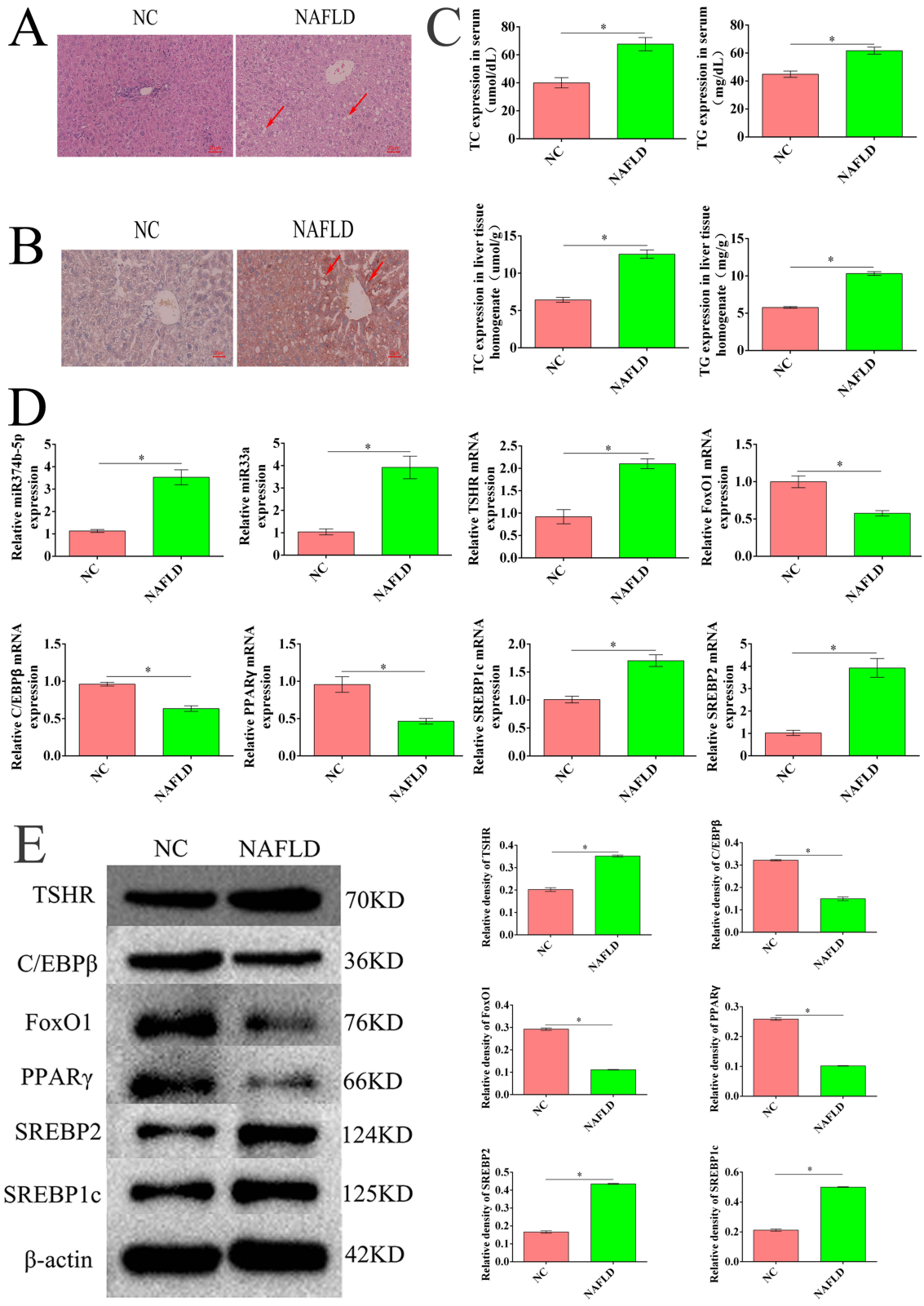

Figure 5 Effect of *miR374b* on the regulation of NAFLD in vivo. (**A**) Liver HE staining in NAFLD mouse model and control group (n=3,Red arrow lipid vacuoles, Scale bar = 50 μm). (**B**) Oil red O staining in NAFLD mouse model and control group (n=3,Red arrow lipid accumulation site, Scale bar = 50 μm). (**C**) Changes of serum and liver tissues TC and TG levels in NAFLD mouse model compared with negative control (n=6, *$P < 0.05$). (**D**) The mRNA expression of *C/EBP β, FoxO1, PPAR γ, SREBP2, SREBP1c*, and *miR33a* in each group compared with normal control (n=3, *$P < 0.05$). (**E**) Western blot showed the expression of TSHR, C/EBPβ, FOXO1, PPARγ, SREBP2, and SREBP1c in each group compared with normal control (n=3, * $P < 0.05$).

https://doi.org/10.2147/HMER.S481687 DovePress

miR374b directly targets *C/EBP β* and its downstream target genes, playing a critical role in regulating lipid metabolism. Overexpression of *miR374b* leads to increased fat accumulation, while its downregulation has the opposite effect, highlighting its essential role in maintaining intracellular lipid balance.

The discovery of *miR374b*'s targeted regulation of *C/EBP β*, a key factor in triglyceride metabolism and NAFLD pathogenesis,[30,31] is particularly significant. C/EBP β as a transcription factor that controls energy metabolism[32] can improve lipid accumulation and metabolism in zebrafish larvae,[33] while FOXO1 is an important regulatory factor for energy balance in dormant embryos and is crucial for lipid metabolism in animals.[34] Increased *miR374b* levels lead to elevated *C/EBP β* expression, whereas knocking down *miR374b* reduces its expression. This study also confirms that *miR374b* regulates the expression of *FOXO1* and its downstream genes. These findings suggest that TSH contributes to NAFLD by influencing *miR374b*'s targeting of *C/EBP β* and its downstream gene regulation, presenting a novel therapeutic target for NAFLD management by modulating *miR374b* activity.

Additionally, this research uncovered that *miR374b*-induced lipid accumulation correlates negatively with lipid metabolism, thereby exacerbating NAFLD. It also examined the role of the TSHR in NAFLD pathogenesis. Findings demonstrated that TSHR is involved in TSH-induced NAFLD, where TSH binding to TSHR enhances *miR374b* transcription, subsequently activating C/EBP β to induce lipid production in adipose tissue, highlighting the therapeutic potential of targeting TSHR to mitigate NAFLD onset.The function of TSHR in NAFLD.TSH binds to TSHR, which activates the expression of miR374b. Resulting in a decrease in the expression levels of miR374b target genes C/EBP β and FOXO 1, thereby regulating the expression of downstream lipid metabolism pathway proteins PPAR γ, SREBP2, and SREBP1c.

Despite these insights, the study has limitations that warrant further investigation. Primarily, it relies on the HepG2 cell line, which might not fully mimic the complex cellular dynamics of human lipid metabolism. Future studies should incorporate primary human liver cells to validate these findings. Additionally, while the findings offer valuable in vitro insights, they require validation in clinical settings to confirm their relevance to NAFLD pathogenesis. Moreover, although it was established that *miR374b* targets *C/EBP β* and *FOXO1*, impacting lipid metabolism in NAFLD, the study did not thoroughly explore the detailed molecular mechanisms and downstream lipid metabolism processes. Further investigations are necessary to elucidate the specific signaling pathways and molecular interactions involved.

Conclusion

These findings suggest that TSHR-induced upregulation of *miR374b* accelerates NAFLD progression by modulating lipid metabolism pathways through C/EBP β and FOXO1, positioning *miR374b* as a potential therapeutic target for NAFLD.

Author Contributions

All authors made a significant contribution to the work reported, whether that is in the conception, study design, execution, acquisition of data, analysis and interpretation, or in all these areas; took part in drafting, revising or critically reviewing the article; gave final approval of the version to be published; have agreed on the journal to which the article has been submitted; and agree to be accountable for all aspects of the work.

Funding

This research was supported by grants from the National Natural Science Foundation of China (81770785 and 82370793) and the Scientific Research Program of Higher Education Institutions in Anhui Province (2023AH040103).

Disclosure

Juyi Li was contributed as first author. The authors report no conflicts of interest in this work.

References

1. Ding L, Oligschlaeger Y, Shiri-Sverdlov R, Houben T. Nonalcoholic Fatty Liver Disease. *Handb Exp Pharmacol*. 2022;270:233–269. doi:10.1007/164_2020_352

2. Duell PB, Welty FK, Miller M, et al. Nonalcoholic Fatty Liver Disease and Cardiovascular Risk: a Scientific Statement From the American Heart Association. *Arterioscler Thromb Vasc Biol*. 2022;42(6):e168–e185. doi:10.1161/ATV.0000000000000153
3. Fan H, Liu Z, Zhang X, et al. Thyroid Stimulating Hormone Levels Are Associated With Genetically Predicted Nonalcoholic Fatty Liver Disease. *J Clin Endocrinol Metab*. 2022;107(9):2522–2529. doi:10.1210/clinem/dgac393
4. Gharib H, Tuttle RM, Baskin HJ, et al. Subclinical thyroid dysfunction: a joint statement on management from the American Association of Clinical Endocrinologists, the American Thyroid Association, and the Endocrine Society. *Endocr Pract*. 2004;10(6):497–501. doi:10.4158/EP.10.6.497
5. Gu Y, Wu X, Zhang Q, et al. High-Normal Thyroid Function Predicts Incident Nonalcoholic Fatty Liver Disease Among Middle-Aged and Older Euthyroid Subjects. *J Gerontol a Biol Sci Med Sci*. 2022;77(1):197–203. doi:10.1093/gerona/glab037
6. Chen YL, Tian S, Wu J, et al. Impact of Thyroid Function on the Prevalence and Mortality of Metabolic Dysfunction-Associated Fatty Liver Disease. *J Clin Endocrinol Metab*. 2023;108(7):e434–e443. doi:10.1210/clinem/dgad016
7. Cui X, Wang F, Liu C. A review of TSHR- and IGF-1R-related pathogenesis and treatment of Graves' orbitopathy. *Front Immunol*. 2023;14:1062045. doi:10.3389/fimmu.2023.1062045
8. Kumar S, Coenen M, Iyer S, Bahn RS. Forkhead Transcription Factor FOXO1 Is Regulated by Both a Stimulatory Thyrotropin Receptor Antibody and Insulin-Like Growth Factor-1 in Orbital Fibroblasts from Patients with Graves' Ophthalmopathy. *Thyroid*. 2015;25(10):1145–1150. doi:10.1089/thy.2015.0254
9. Vidal-Cevallos P, Murua-Beltran Gall S, Uribe M, Chavez-Tapia NC. Understanding the Relationship between Nonalcoholic Fatty Liver Disease and Thyroid Disease. *Int J Mol Sci*. 2023;24(19):14605. doi:10.3390/ijms241914605
10. Hochreuter MY, Dall M, Treebak JT, Barres R. MicroRNAs in non-alcoholic fatty liver disease: progress and perspectives. *Mol Metab*. 2022;65:101581. doi:10.1016/j.molmet.2022.101581
11. Mahmoudi A, Butler AE, Jamialahmadi T, Sahebkar A. The role of exosomal miRNA in nonalcoholic fatty liver disease. *J Cell Physiol*. 2022;237(4):2078–2094. doi:10.1002/jcp.30699
12. Latorre J, Moreno-Navarrete JM, Mercader JM, et al. Decreased lipid metabolism but increased FA biosynthesis are coupled with changes in liver microRNAs in obese subjects with NAFLD. *Int J Obes Lond*. 2017;41(4):620–630. doi:10.1038/ijo.2017.21
13. Yu Y, Tian T, Tan S, et al. MicroRNA-665-3p exacerbates nonalcoholic fatty liver disease in mice. *Bioengineered*. 2022;13(2):2927–2942. doi:10.1080/21655979.2021.2017698
14. Qiao JT, Cui C, Qing L, et al. Activation of the STING-IRF3 pathway promotes hepatocyte inflammation, apoptosis and induces metabolic disorders in nonalcoholic fatty liver disease. *Metabolism*. 2018;81:13–24. doi:10.1016/j.metabol.2017.09.010
15. Lebeaupin C, Vallee D, Hazari Y, Hetz C, Chevet E, Bailly-Maitre B. Endoplasmic reticulum stress signalling and the pathogenesis of non-alcoholic fatty liver disease. *J Hepatol*. 2018;69(4):927–947. doi:10.1016/j.jhep.2018.06.008
16. Azzimato V, Chen P, Barreby E, et al. Hepatic miR-144 Drives Fumarase Activity Preventing NRF2 Activation During Obesity. *Gastroenterology*. 2021;161(6):1982–1997e11. doi:10.1053/j.gastro.2021.08.030
17. Ghareghani P, Shanaki M, Ahmadi S, et al. Aerobic endurance training improves nonalcoholic fatty liver disease (NAFLD) features via miR-33 dependent autophagy induction in high fat diet fed mice. *Obes Res Clin Pract*. 2018;12(Suppl 2):80–89. doi:10.1016/j.orcp.2017.01.004
18. Long JK, Dai W, Zheng YW, Zhao SP. miR-122 promotes hepatic lipogenesis via inhibiting the LKB1/AMPK pathway by targeting Sirt1 in non-alcoholic fatty liver disease. *Mol Med*. 2019;25(1):26. doi:10.1186/s10020-019-0085-2
19. Wang Z, Zhu Y, Xia L, Li J, Song M, Yang C. Exercise-Induced ADAR2 Protects against Nonalcoholic Fatty Liver Disease through miR-34a. *Nutrients*. 2022;15(1):121. doi:10.3390/nu15010121
20. Zhang T, Duan J, Zhang L, et al. LXRalpha Promotes Hepatosteatosis in Part Through Activation of MicroRNA-378 Transcription and Inhibition of Ppargc1beta Expression. *Hepatology*. 2019;69(4):1488–1503. doi:10.1002/hep.30301
21. He Y, Rodrigues RM, Wang X, et al. Neutrophil-to-hepatocyte communication via LDLR-dependent miR-223-enriched extracellular vesicle transfer ameliorates nonalcoholic steatohepatitis. *J Clin Invest*. 2021;131(3). doi:10.1172/JCI141513
22. Pan S, Zheng Y, Zhao R, Yang X. miRNA-374 regulates dexamethasone-induced differentiation of primary cultures of porcine adipocytes. *Horm Metab Res*. 2013;45(7):518–525. doi:10.1055/s-0033-1334896
23. Vieira IH, Rodrigues D, Paiva I. The Mysterious Universe of the TSH Receptor. *Front Endocrinol*. 2022;13:944715. doi:10.3389/fendo.2022.944715
24. Zhou W, Brumpton B, Kabil O, et al. GWAS of thyroid stimulating hormone highlights pleiotropic effects and inverse association with thyroid cancer. *Nat Commun*. 2020;11(1):3981. doi:10.1038/s41467-020-17718-z
25. Refetoff S. Resistance to thyroid hormone and its molecular basis. *Acta Paediatr Jpn*. 1994;36(1):1–15. doi:10.1111/j.1442-200x.1994.tb03121.x
26. Walczak K, Sieminska L. Obesity and Thyroid Axis. *Int J Environ Res Public Health*. 2021;18(18):9434. doi:10.3390/ijerph18189434
27. Postiglione MP, Parlato R, Rodriguez-Mallon A, et al. Role of the thyroid-stimulating hormone receptor signaling in development and differentiation of the thyroid gland. *Proc Natl Acad Sci U S A*. 2002;99(24):15462–15467. doi:10.1073/pnas.242328999
28. Yan F, Wang Q, Lu M, et al. Thyrotropin increases hepatic triglyceride content through upregulation of SREBP-1c activity. *J Hepatol*. 2014;61(6):1358–1364. doi:10.1016/j.jhep.2014.06.037
29. Liu YY, Heymann RS, Moatamed F, Schultz JJ, Sobel D, Brent GA. A mutant thyroid hormone receptor alpha antagonizes peroxisome proliferator-activated receptor alpha signaling in vivo and impairs fatty acid oxidation. *Endocrinology*. 2007;148(3):1206–1217. doi:10.1210/en.2006-0836
30. Lee J, Jung E, Lee J, et al. Isorhamnetin represses adipogenesis in 3T3-L1 cells. *Obesity*. 2009;17(2):226–232. doi:10.1038/oby.2008.472
31. Kim MS, Baek JH, Lee J, Sivaraman A, Lee K, Chun KH. Deubiquitinase USP1 enhances CCAAT/enhancer-binding protein beta (C/EBPbeta) stability and accelerates adipogenesis and lipid accumulation. *Cell Death Dis*. 2023;14(11):776. doi:10.1038/s41419-023-06317-7
32. Janardhan HP. The HIF-1 alpha-C/EBP alpha axis. *Sci Signal*. 2008;1(43):jc2. doi:10.1126/scisignal.143jc2
33. Ajay G, Gokul S, Namasivayam SKR, et al. Serine Threonine-Protein Kinase-Derived IW13 Improves Lipid Metabolism via C/EBP-alpha/SREBP1/FAS Signaling Pathways in HFD-Induced Zebrafish In Vivo Larval Model. *Appl Biochem Biotechnol*. 2023;195(8):4851–4863. doi:10.1007/s12010-023-04480-3
34. van der Weijden VA, Stotzel M, Iyer DP, et al. FOXO1-mediated lipid metabolism maintains mammalian embryos in dormancy. *Nat Cell Biol*. 2024;26(2):181–193. doi:10.1038/s41556-023-01325-3